

# Measuring Starlight Deflection during the 2017 Eclipse: Repeating the Experiment that made Einstein Famous

*Donald Bruns*  
7387 Celata Lane  
San Diego, CA 92129  
*dbruns@stellarproducts.com*

*George Kaplan*  
US Naval Observatory  
Washington, D.C. 20392

*Al Nagler*  
Tele Vue Optics, Inc.  
Chester, NY 10918

*Greg Terrance*  
Finger Lakes Instrumentation  
Lima, NY 14485

---

## Abstract

In 1919, astronomers performed an experiment during a solar eclipse, attempting to measure the deflection of stars near the sun, in order to verify Einstein's theory of general relativity. The experiment was very difficult and the results were marginal, but the success made Albert Einstein famous around the world. Astronomers last repeated the experiment in 1973, achieving an error of 11%. In 2017, using amateur equipment and modern technology, we plan to repeat the experiment and achieve a 1% error. The best available star catalog will be used for star positions. Corrections for optical distortion and atmospheric refraction are better than 0.01 arcsec. During totality, we expect 7 or 8 measurable stars down to magnitude 9.5, based on analysis of previous eclipse measurements taken by amateurs. Reference images (taken near the sun during totality) will be used for precise calibration. Preliminary test runs performed during twilight in April 2016 and April 2017 can accurately simulate the sky conditions during totality, providing an accurate estimate of the final uncertainty.

---

## 1. Introduction

Albert Einstein published his theory of general relativity in 1915, and soon made the startling prediction that the sun's gravity would deflect light twice as much as Newtonian physics indicated. He calculated that the deflection of light from a star appearing just at the edge of the sun would be about 1.7 arcseconds, making it appear slightly shifted. This is shown diagrammatically in Figure 1.

Sir Arthur Eddington proposed that this miniscule deflection could be measured during a solar eclipse, and several expeditions were attempted before success at the 1919 eclipse. Those early measurements were not very accurate, however [Will 2015; Kenefick

2009], and later measurements had only a slight improvement [Will 2010, Will 2014; Friesen 2011] as shown in Figure 2.

The most recent attempt [Brune 1976; Jones 1976], organized by the University of Texas, required moving 6 tons of equipment to Africa and leaving it there for 6 months in a guarded shed. The telescope was a 200 mm aperture refractor with a 2.1 meter focal length. The images were recorded on 12" glass plates. This was a heroic experiment, but only achieved an 11% uncertainty; with today's technology, a better result should be obtained with a much smaller effort. Since radio telescope observations have made ultra-precise measurements of deflection down to 0.0002 arcsec, this new experiment is simply a celebration of the original experiment.

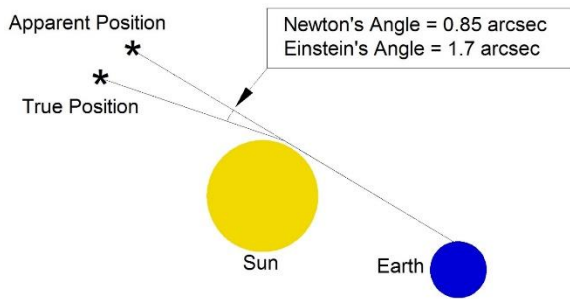


**Figure 1.** The apparent position of a star seen near the edge of the sun is deflected by a very small amount, depending on which theory is used in the calculation.

In order to measure the deflection of light by the sun's gravity, an experiment needs to be set up very carefully. Basically, three things are needed:

1. Get good images with some bright stars,
2. Determine where the stars should be, and
3. Calculate the difference to get deflection.

This requires a very good telescope, a very good camera, and very good experimental design. To measure the difference between the expected and measured location of the stars in the image requires a very good star catalog with several small, but important corrections. Finally, the location of the stars in the images need to be measured with a very small uncertainty, ultimately reaching an average error of only 0.01 arcsec. With today's technology, CCD cameras can replace glass plates, image processing software can replace scanning micro-densitometers, and satellite-measured catalogs eliminate the problem of measuring the stars six months before or after the eclipse. This makes the experiment much simpler and should lead to much higher precision.

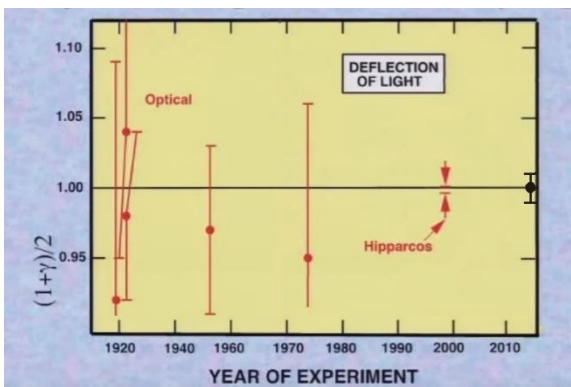


**Figure 2.** The deflection of light has been measured during a total eclipse only a few times in the last century. Hipparcos measured the deflection from space, not needing an eclipse, and has set the record for the most precise optical measurement. The marker on the right side of the graph represents the expected error of 1% for our 2017 experiment. Modified from [Will 2015]. Vertical scale is deflection normalized to Einstein's calculation.

## 2. Equipment and Experiment Design

### 2.1 Telescope

This experiment is made feasible by the availability of superb, commercially-available amateur astronomy equipment. Some of these items were not even dreamed of in 1973, and have been vastly improved even since the 2006 eclipse. By carefully analyzing all of the requirements for this experiment and comparing those requirements with a wide variety of telescopes and cameras, the optimum combination was selected.

The ideal telescope is the Tele Vue NP101is refractor, shown in Figure 3 [www.televue.com]. This telescope is small enough to be portable, but its 101 mm aperture is large enough to capture 10<sup>th</sup> magnitude stars with 1 second exposures. Its diffraction limit is only 1.3 arcsec at 630 nm, much smaller than the 2.5 arcsecond daytime seeing we expect to encounter. The short focal length of only 540 mm allows a wide field of view.



**Figure 3.** The Tele Vue NP101is telescope provides essentially perfect optics over a flat, wide field of view, all necessary to provide good images during the eclipse. The short focal length provides an ideal size match to the imaging camera pixels.

We've used this same telescope model in previous experiments, and have always verified that its optical performance is essentially perfect. The image plane is flat and color-free, with no central obscuration or spider to add scatter. This makes the telescope a very-high contrast instrument.

Al Nagler of Tele Vue provided optical distortion measurements in red light for this model, amounting to only 0.05% at 1.2°. While this is small enough to ignore for most wide-field imaging applications, it might be one of the biggest error sources in the final experiment. The rugged, lockable focuser allows us to take images a few minutes before and after totality, with minimum risk of camera movement. This stability allows good calibration to remove the distortion effect.

### 2.2 Camera

Once the telescope was chosen, a wide variety of astronomical cameras were reviewed against the experimental requirements. The clear winner was the

monochrome Microline 8051 CCD camera from Finger Lakes Instrumentation [www.flicamera.com] shown in Figure 4. An interline CCD sensor was required so that no mechanical shutter was needed. A large format sensor was desirable, but too many pixels would require too much time to digitize the images. Since totality only lasts 140 seconds, this speed is critical. A larger format camera might image more stars, but the number of stars per second is optimized for the 8 MPixel 8051 model. This sensor's pixels are only 5.5 microns wide, a perfect match for the NP101is telescope focal length, giving 2.1 arcseconds per pixel. While this pixel size has a moderate size full-well capacity, the resolution requirement is more important. It turns out that the stars in the neighborhood of the sun during totality have a small range of magnitudes (7.4 to 9.5), so the dynamic range is not too important. Exposures will be bracketed to make sure at least one-third of the frames are useable, so this also mitigates the dynamic range concern.



**Figure 4.** The Finger Lakes Instrumentation Microline ML8051 camera uses 12MHz digitizing speed for a fast frame rate with low readout noise. The interline CCD sensor does not require a mechanical shutter, so vibrations and delays are minimized.

This ML8051 camera digitizes at 12 MHz, so digitizing a full frame takes only 0.7 seconds. If the exposures range from 0.2 seconds to 1 second, then over 100 images can be saved during this short eclipse.

The camera will be cooled to reduce readout noise, but since it will be operated during the daytime, the focal plane temperature might not fall much below 0° C. The background signal noise will probably overwhelm the readout noise or dark current noise, but temperature stability during the eclipse and the calibration phase is very important. The built-in fan will be operated at a reduced speed to minimize any vibration.

The camera is mounted with a T-mount flange that mates directly with the 2.4" diameter Tele Vue focuser. This makes the camera mounting very stable, further reducing any camera-telescope drift.

### 2.3 Mount

The telescope mount needs to be set up and polar aligned before the eclipse, and hopefully, the weather will cooperate so this can be done the previous night. A portable mount is required that can handle the NP101is and the FLI ML8051 camera. The Software Bisque [www.bisque.com] MyT Paramount, shown in Figure 5 on its standard field tripod, meets this requirement. The particular mount to be used in this experiment has a periodic error correction only a few arcseconds, and with permanent PEC, the tracking error was measured less than one arcsecond. Setting up this mount in the daytime might be required, but can be done to less than one degree polar alignment error using the built-in scales and using a hand-held GPS to determine true north. This amount of polar error creates only about 1/4 arcsecond tracking error per 1 second exposure, smaller than the errors due to seeing or diffraction. Tracking error can be ignored, but a nighttime polar alignment will make eclipse-day automation less risky.



**Figure 5.** The Software Bisque MyT Paramount and matching tripod is portable, allowing a change in eclipse sites in case of bad weather. The periodic error, after correction, is sub-arcsecond, necessary for high quality images.

## 2.4 Sky brightness data near the sun

Since this eclipse has only 140 seconds of totality, there is no time to experiment with different exposures. Fortunately, there is one example of calibrated brightness near the sun [Viladrich 2016]. We used this data to predict what to expect during the eclipse.

An important pre-eclipse issue is to determine which stars can be seen during totality. After looking at hundreds of eclipse photos from dozens of posted web sites, we were able to find only one eclipse chaser who used an astronomical camera to image during totality. Fortunately, he also took dark frames, used a monochrome sensor, and saved his files in FITS format. Christian Viladrich of France used an SBIG STL-11000 camera during the March 2006 eclipse from Egypt, using a similar telescope. His exposures were only 5 msec long, since he wanted to image the inner part of the corona. We first stretched his images by factors of 40 and 200 to get simulated images of 200 msec and 1 second. Ignoring CCD blooming, we then estimated the background brightness levels near the sun, and calculated how bright a star would be visible. The calculations included the noise due to the background light over a small number of pixels and then estimated the signal-to-noise ratio (SNR) for the different stars in the field of view. Since we need to accurately measure the centroid of the star, we required the calculated centroid error be less than 0.1 arcsec, leading to a minimum SNR of 16. The results are illustrated in the next figure. While more than 60 stars brighter than magnitude 12 are in the field of view, we hope to get good measurements from 7 or 8 stars with a limiting magnitude of 9.5. Note that the sun is offset from center in order to maximize the number of measureable stars.

The two stars that appear closest to the sun will have a larger gravitational deflection, about 1.2 arcseconds. However, the corona will be variable and the sloping background might make those measurements unreliable. The average deflection of the dimmer stars that fall near the edge of the field of view is only about 0.4 arcsec, but appear on a flatter background. Since the FLI Microline camera downloads images in less than one second and no mechanical shutter is required, the plan is to take as many images as possible with both exposure durations.

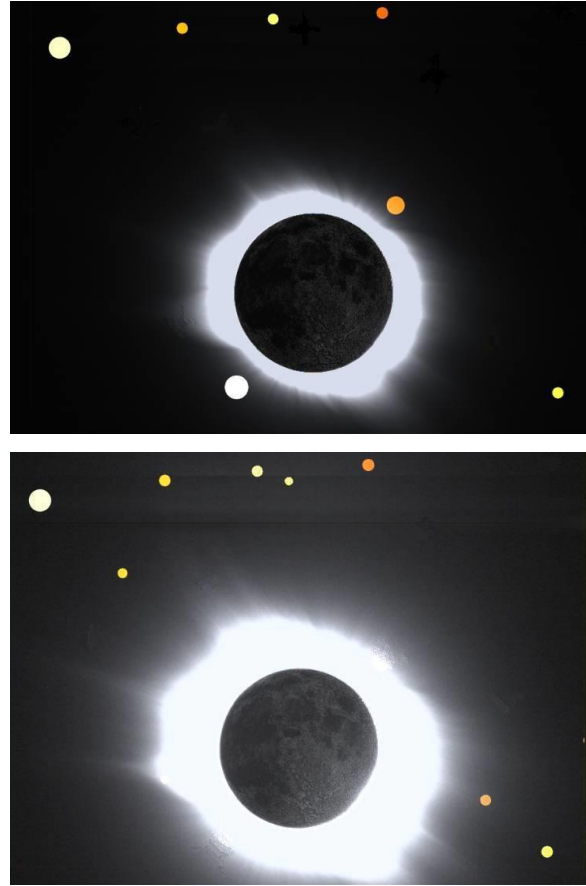


**Figure 6. Total eclipse image from Viladrich, stretched and superimposed on measureable stars. The top image is a simulated 200 msec exposure, and allows two bright stars near the sun to be measured. The bottom image is a simulated exposure of 1 second, so the corona masks the nearby stars while allowing three dimmer stars to appear.**

## 2.5 Zenith sky brightness

During the partial eclipse phases before and after totality, there have been a few measurements of overall or zenith sky brightness [Sharp 1971; Silverman 1975; Möllmann 2006; Zainuddin 2009; Strickling 2016]. If the sky is dark enough, then some star fields near the sun could be imaged to provide the necessary calibration data. Dozens of stars in each image are needed to measure the precise plate scale and the precise optical axis, but this is not possible until totality, based on the following analysis.

Figure 7 shows the sky brightness during several eclipses, measured using all-sky photometers. There is a wide variation in brightness, but the conclusions don't change. The sky brightness has been converted to a visible star magnitude, normalized to magnitude 9.5 for the time during totality. Even one minute from totality, the stars need to be magnitude 4 or 5 to be

visible. Even the Pleiades cluster might show only five stars, too few to do a reliable calibration. Unfortunately, this means that reference star fields need to be imaged during precious totality time.

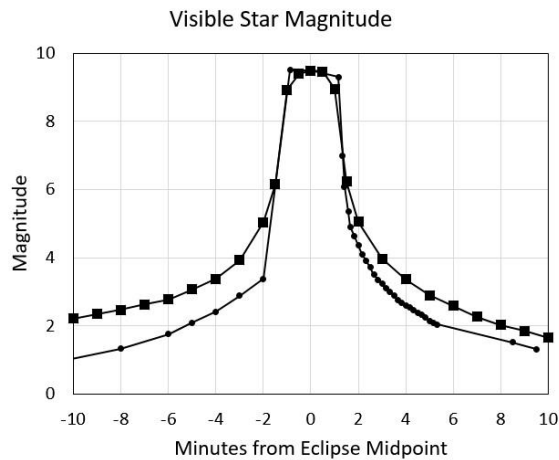


**Figure 7.** Sky brightness data from two eclipses show that only bright stars are visible outside of the two-minute totality period. Squares are from Möllmann and Vollmer, (2006); dots are from Strickling (2016). Data points are normalized to magnitude 9.5 during totality.

Two reference star fields are required during the brief totality phase; one series taken before the eclipse field, and one taken afterward, on opposite sides of the sun. Immediately after totality, while the sky is still slightly darkening, the first reference field is imaged 15 times in 30 seconds. The frame is shown on the right side of Figure 8. The figure is shown parallel to the sky's right ascension axis, and should be rotated counterclockwise by  $27^\circ$  for correct orientation with the horizon. This makes this reference field slightly higher in elevation, but the telescope orientation with respect to the horizon is nearly fixed, minimizing flexure changes. This star field is about  $8^\circ$  west of the sun, far enough so that it is sure to be darker. The gravitational deflection is fairly constant across the field, ranging from about 0.07 arcsec to 0.05 arcsec. This particular star field was chosen because it has a large number of stars within a small brightness range, so all of the stars should be measureable.

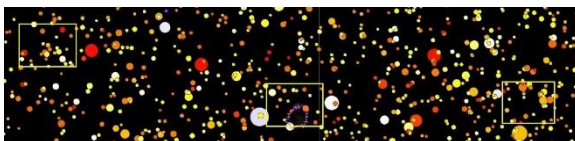


**Figure 8.** The two reference fields to be imaged during the eclipse are approximately equally spaced on either side of the central eclipse field. This allows the average calibration based on those two reference fields to accurately represent the eclipse field.

The first reference field imaging will start just after totality. Then, 30 seconds later, the telescope will be repointed to the central eclipse field. This is the darkest part of totality, but exposures will be bracketed to insure at least some usable images. After 60 seconds imaging the central eclipse field, the telescope will be repointed to the second reference field for the last 30 seconds of totality, about  $8^\circ$  east of the sun. This field is shifted slightly in declination, again simply to maximize the number of measureable stars. The shift is minor, and is in the direction to minimize the effects of refraction. The field is also not too far from the meridian, to avoid a meridian flip in the MyT Paramount that would take 30 seconds. The time needed to move the telescope from the eclipse field to either reference field, then re-start tracking, is measured at about 3 seconds. Half of the total eclipse time is spent on the reference fields and half of the time on the eclipse field. This reduces the risk in the final analysis.

One additional requirement in the experimental plan is to make sure the telescope is focused as well as the seeing allows. This maximizes the star's SNR. While focusing on stars during setup on the previous night will give a good starting point, changes in temperature will require a small adjustment, especially since the depth of focus for the Tele Vue NP101 is only about  $\pm 2 \cdot \lambda \cdot (\text{focal ratio})^2$ , or  $\pm 37$  microns for red light. Fortunately, the focuser can easily achieve this resolution using its 10:1 fine focus knob, and locking the focus does not change the distance. The requirement is to find an appropriate star upon which to focus. Based on the curves in Figure 7, magnitude +0.5 Procyon should be visible at least 10 minutes before totality. It is only  $36^\circ$  from the sun, at nearly the same altitude, and will not require a meridian flip. This makes it a perfect target with plenty of time to spare.

### 3. Star Positions

#### 3.1 Star catalog choices

All previous eclipse experiments required imaging the same star field six months before or after the eclipse, in order to determine the un-deflected star positions to sub-arcsecond accuracy. Parallax was not important, since the geometry of the sun and the earth was the same. This was one of the most challenging parts of their experiments, since the telescope and camera had to be left un-touched for six months in order to minimize mechanical errors. The tests were done at night; the temperature was different, and this also had to be corrected.

Since then, the Hipparcos satellite has provided a very good astrometric reference catalog, apparently



obviating the need to measure stars before or after the eclipse. However, since those measured positions are now 25 years old, the uncertainties for the best stars, the Tycho-2 subset, are typically 0.1 arcsec, as shown in Figure 9. This is not nearly good enough for this experiment, but is widely available and in use by almost all commercial planetarium programs. Fortunately, there are two work-arounds.

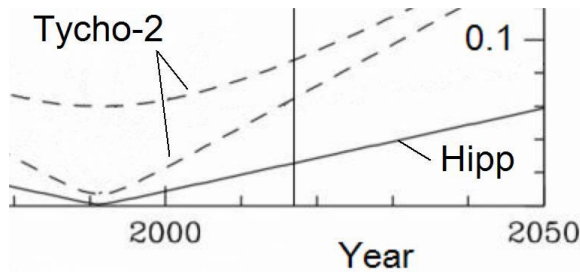


**Figure 9. Star position accuracy has degenerated since 1991. The curve labeled Hipp is for only a limited number of bright stars, so does not apply to most of the stars for this experiment. The lower curve marked Tycho-2 is for some select bright stars; most of the Tycho-2 catalog stars follow the upper curve. The vertical line at 2017 indicates that most stars have an uncertainty near 0.1 arcsec. Figure adapted from Michael Perryman - Own work, CC BY-SA 3.0, <https://commons.wikimedia.org/w/index.php?curid=5521856>**

The USNO just released their URAT1 catalog last year, with typically 10 milliarcsecond measurement errors. Since only 2.5 years would elapse between the catalog epoch and the 2017 eclipse, this solves most of the problems. Unfortunately, the URAT1 catalog does not include parallax. This makes the position too uncertain for nearby bright stars, unless the right geometry is used. During the eclipse, the stars are in line with the sun, so the parallax is essentially zero. To calibrate telescope optical distortion at night, images must be taken near local midnight and near the meridian, so the parallax is again near zero. For other tests, only the brighter stars can be used, whose measured parallax values can be copied from older catalogs. In September of 2016, however, the situation becomes dramatically better.

The ESA Gaia satellite is the newest generation of astrometric satellites. It was just launched in 2013, and is in the middle of measuring a billion stars with an accuracy of 0.000024 arcseconds. Since it is still measuring stars, it has not had enough time to measure parallax or proper motion. The ESA has decided, however, to release the first catalog at the end of the summer of 2016! This first catalog will combine the measurements from the Tycho-2 catalog to get very accurate proper motions and parallax numbers. This will be the ultimate solution, just in time for the 2017 eclipse. Everyone is hoping that this schedule can be maintained, so we are anxiously awaiting the results.

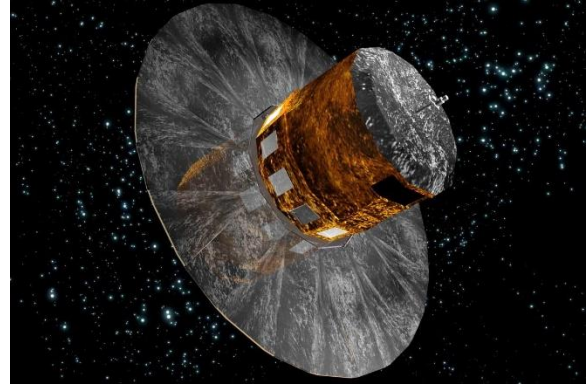


**Figure 10. The Gaia satellite is now measuring stars with micro-arcsecond precision, and ESA will release the first catalog just in time for the 2017 experiment.**

### 3.2 Refraction corrections

The precise apparent positions of stars depends on their catalog positions, modified by proper motion, parallax, precession, nutation, stellar aberration, solar gravitational deflection, and local atmospheric refraction [Kaplan 1989]. Rigorous software to combine all of these features was developed by the US Naval Observatory, by the astronomers who co-produce the *Astronomical Almanac* and the *Nautical Almanac*. The program is called NOVAS, for Naval Observatory Vector Astrometry Software [Kaplan 2011], and is free to download. It comes in FORTRAN, C, and Python language editions, so one of those compilers needs to run on the user's computer. The posted NOVAS version 3.1 uses only a simple subroutine to correct for refraction, so we incorporated a more precise routine based on the work of Stone [Stone 1996], also of the USNO (Flagstaff Station). Our modified program now outputs stellar positions corrected to a relative refractive error of 0.005 arcsec.

To maintain this precision, we will monitor the local air temperature to within  $\pm 2^\circ$  F and the atmospheric pressure to within 3 millibars. The FAA weather station nearest the eclipse site can provide the air pressure normalized to sea level, so we will correct it back to the actual pressure at the site's elevation. We will also measure the air temperature near the telescope with a fast-response thermometer. Since the air temperature falls during the eclipse, an ordinary thermometer won't work; Bruns designed an electronic thermometer with a 1-second response time in air accurate to  $0.2^\circ$  F, and we will make a recording of the temperature during the entire eclipse. These efforts should make the apparent star positions much better than required.

### 3.3 Geometric lens distortion

All telescopes suffer from lens distortion, since the optical designer prefers to minimize coma, spherical aberration, astigmatism, and field curvature. Fortunately, this geometric distortion can be easily corrected in post-processing. All that is needed is a good measurement of the magnitude of the distortion. However, it turns out that this correction may be the most significant error source in the experiment because locating the precise optical center is difficult.

From optical raytracing, a pretty good estimate of the distortion was provided by Nagler for the NP101is telescope. We then fit the distortion values he provided to a simple quadratic curve so we could predict the distortion for any star in the field of view. By taking images near the zenith at night, the measured distortion was compared to the calculated distortion with very good agreement. The coefficients in the polynomial curve are not expected to change over temperature or focus, and these will be verified for this telescope before the eclipse date. Hopefully, once measured, a simple check on the reference fields on eclipse day will be all that is needed to make star position corrections reliably down to the 0.01 arcsecond level.

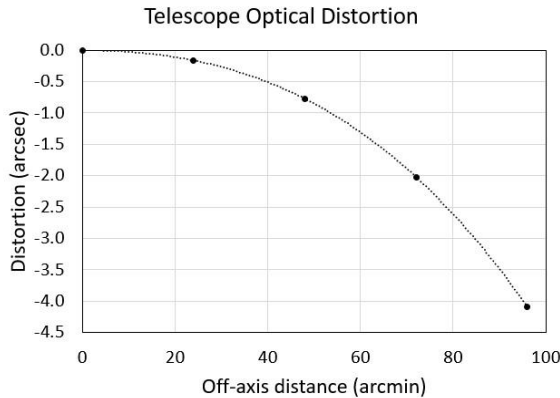


**Figure 11. The optical distortion for the Tele Vue refractor amounts to 2 arcsec at the corners of the image. This must be reduced by a factor of 100 to meet the precision requirements of the experiment. A small change in the location of the optical axis makes a big difference in the distortion correction.**

However, the distortion varies as the square of the distance from the optical axis, and many of the stars are at large distances from the CCD center. Hence, the corrections are very dependent on the precise location of the optical axis on the CCD. In fact, if the optical axis moves only 25 microns from the calibrated position, the error in location will be off by 0.01 arcsec. A 50 micron error from the calibrated position affects the star correction by 0.02 arcsec, so the effect is linear. The important question here is how to either insure

that the camera location does not change by more than 25 microns (4.5 pixels on the focal plane), or determine some technique to measure it. Using the reference field data and fitting the star location to the expected (distorted) positions is the simplest method. Since reference fields will be taken on either side of the sun during totality, the location of the optical axis can be averaged to get the location for the eclipse images. This technique, along with others, is currently being tested.

### 4. Image Analysis

After the eclipse images are ready (dark-frame and flat field corrected), the star locations need to be accurately measured. In past astrometric programs, MaximDL has been used in manual mode. Since there may be only a few hundred stars to measure, this is one option. Each star can be examined to make sure there are no image artifacts, like cosmic rays, that might skew that star's location. For the calibration data and reference data, however, there might be thousands of stars, so some automation is beneficial. In this case, a few bad stars might be ok, since they will be averaged out. The image processing software must be able to measure the star location to 0.01 pixels.

There are several standard methods to determine star locations [Stone 1898; Mighell 1999; Thomas 2004]. The most accurate techniques include simple barycentric calculations and Gaussian curve fitting. The barycentric technique multiplies the intensity of each pixel by its coordinates, and then divides by total intensity. This calculation can be affected by noise, but works for cases where most of the signal is contained in just four pixels. The alternate method fits a 3-D Gaussian curve to the pixel intensities, mathematically looking for the best fit. The location of the Gaussian center is reported as the star location. When only a few pixels are illuminated, this technique is also subject to errors. One improvement would be to constrain the test-Gaussian curve diameter to be the same for every star, but this software is yet to be developed.

Automated software programs, including Pinpoint, Prism, and Astrometrica, were used in the preliminary data analysis. The main problem here is that they use the outdated star catalogs to perform the measurements, leading to small, but important errors. By the time of the 2017 eclipse, we hope to have developed some custom software.

### 5. Preliminary tests

While there is a range of measurements, the consensus is that the sky during totality is about as bright as when the sun is  $5.5^\circ$  below the horizon. The most

accurate preliminary test is to image the three star fields during those particular few moments of twilight, and when the star fields are approximately at the same elevation. Fortunately, this occurs in late March and early April. The test included the same exposure durations and timing as in the real eclipse. This data will be processed in the next few months using the same software, and the results compared with the best star catalogs. The results should show a gravitational deflection of zero, of course, since the sun is far away. The uncertainty in the measurements is expected to be on the order of 0.01 arcsec, slightly better than that expected during the eclipse. This proves the technique and gives confidence in the 2017 experiment. Once the Gaia catalog is available, the data may be re-processed. A second dry run will be performed in April 2017, as a final test for eclipse day only four months later.

## 6. Observation location

The site for the experiment is likely in Wyoming, but a site-selection trip is planned for this August, with the hope that the weather will be similar in 2017. The notorious winds of Wyoming are a concern, not just for the stability of the equipment, but also because the air quality might be affected. The increased transparency for the high altitudes in Wyoming might be degraded by dust stirred up by the wind. Fortunately, modern technology again offers the benefit of pretty accurate 48-hour weather forecasts, so moving the experiment will be easier.

## 7. Conclusions

This experiment repeats the measurements that made Einstein famous. It is a very difficult experiment because all predictions must come true and no hidden errors must be overlooked. Modern technology, including essentially perfect wide-field telescopes and high speed CCD cameras, along with accurate star catalogs, make this a much simpler experiment than any previous attempts. The anticipated results will also be far more accurate than any previous ground-based attempt. Whether or not this experiment goes as planned, the next USA opportunity will be in Texas in 2024.

## 8. Acknowledgements

While this experiment was primarily the responsibility of the lead author, he received critical help and aid from a wide variety of friends and associates. He wishes to thank John Bangert of USNO for advice on URAT1, Suresh Rajgopal for assistance in setting up

NOVAS and Christian Viladrich for his 2006 eclipse FITS image files.

## 9. References

Brune, R.A. Jr. and the Texas Mauritanian Eclipse Team, "Gravitational deflection of light: solar eclipse of 30 June 1973 I. Description of procedures and final results" (1976). *A.J.* **81**, 452-454.

Friesen, J., A. Rogers, and J.D. Fiege, "Challenging Einstein: Gravitational Lensing as a Test of General Relativity" (2011). *JRASC* **105**, 61-65.

Jones, B.F. "Gravitational deflection of light: solar eclipse of 30 June 1973 II. Plate reductions" (1976). *A.J.* **81**, 455-463.

Kaplan, G.H., J.A. Hughes, P.K. Seidelmann, C.A. Smith, and B.D. Yallop, "Mean and Apparent Place Computations in the new IAU System. III. Apparent, Topocentric, and Astrometric Places of Planets and Stars" (1989). *A.J.* **97**, 1197-1210.

Kaplan, G., J. Bartlett, A. Monet, J. Bangert, and W. Puatua, (2011) User's Guide to NOVAS Version F3.1 (Washington, DC: USNO).

Kennefick, D., "Testing relativity from the 1919 eclipse – a question of bias" (2009). *Physics Today* **March 2009**, 37-42.

Mighell, K.J., "Algorithms for CCD Stellar Photometry" (1999). *ASP* **172**, 317-328.

Möllmann, K.-P. and M. Vollmer, "Measurements and predictions of the illuminance during a solar eclipse" (2006). *Eur.J.Phys.* **27**, 1299-1314.

Sharp, W.E., S.M. Silverman, and J.W.F. Lloyd, "Summary of Sky Brightness Measurements During Eclipses of the Sun" (1971). *Applied Optics* **10**, 1207-1210.

Silverman, S.M. and E.G. Mullen, "Sky brightness during eclipses: a review" (1975). *Applied Optics* **14**, 2838-2843.

Stone, R.C. "A comparison of digital centering algorithms" (1989). *A.J.* **97**, 1227-1237.

Stone, R.C., "An Accurate Method for Computing Atmospheric Refraction" (1996). *P.A.S.P.* **108**, 1051-1058.



Strickling, W., <http://www.strickling.net/astro.htm>, accessed March 4, 2016.

Thomas, S., "Optimized centroid computing in a Shack-Hartmann sensor" (2004). *Proceedings of the SPIE* **5490**, 1238-1246.

Viladrich, C., <http://christian.viladrich.perso.neuf.fr/>, accessed March 4, 2016.

Will, C.M., "Resource Letter PTG-1: Precision Tests of Gravity" (2010). *Am.J.Phys.* **78**, 1240-1248.

Will, C.M., "The Confrontation between General Relativity and Experiment" (2014). *Living Rev. Relativity* **17**, 4-117.

Will, C.M. "The 1919 measurement of the deflection of light" (2015). *Class.Quantum Grav.* **32**, 1-14.

Zainuddin, M.Z., S. Haron, M.A. Niri, N. Ahmad, M.S.A.M. Nawawi, S. Man, M.Z. Rodzali, R. Ramli, R.A. Wahab, K. Ismail, and N.H.A. Zaki, "Sky Brightness Condition During Total Solar Eclipse on July 22, 2009" (2013). *Middle-East Journal of Scientific Research* **13**, 220-223.